

PAPER • OPEN ACCESS

## Evidence for Jahn-Teller effects in endohedral fullerenes

To cite this article: Janette L Dunn and Effat Rashed 2018 *J. Phys.: Conf. Ser.* **1148** 012003

View the [article online](#) for updates and enhancements.



**IOP | ebooks™**

Bringing you innovative digital publishing with leading voices to create your essential collection of books in STEM research.

Start exploring the [collection](#) - download the first chapter of every title for free.

# Evidence for Jahn-Teller effects in endohedral fullerenes

**Janette L Dunn and Effat Rashed**

School of Physics & Astronomy, University of Nottingham, University park, Nottingham, NG7 2RD, UK

E-mail: [janette.dunn@nottingham.ac.uk](mailto:janette.dunn@nottingham.ac.uk)

**Abstract.** Endohedral fullerenes can be formed by encapsulating one or more atom or molecule inside the cavity of the fullerene molecule. When a light molecule is encapsulated, it will remain close to the centre of the fullerene molecule without any strong interactions with its environment. This allows the quantum-mechanical behaviour of the molecule to be probed almost as if it were a free molecule. However, energy levels deduced from inelastic neutron scattering (INS) and in infrared spectroscopy show some small splittings compared to the expected results for a free molecule. This indicates that the encapsulated molecule is not totally free from the effects of its environment. More specifically, the molecule must feel an environment that has a lower symmetry than that of an undistorted fullerene cage. We will review the evidence for symmetry-lowering in different types of endohedral fullerenes, and discuss whether the symmetry-lowering could be due to the Jahn-Teller (JT) effect. We will then present some results of a model for  $\text{H}_2\text{O}@C_{60}$  which shows that the splittings seen in INS data could be explained in terms of JT distortions of the encapsulating fullerene cage. Nevertheless, the possibility that they could also be explained with a non-JT model can't be ruled out.

## 1. Introduction

Atoms, ions or molecules can be inserted into the hollow core of a fullerene molecule to produce endohedral fullerenes. These are also called endofullerenes or, when it is a metal atom that is encapsulated, metallofullerenes. Efforts to synthesise endohedral fullerenes were first made soon after it was discovered that  $C_{60}$  had a closed-cage structure [1, 2]. In fact, doping with La ions played an important role in supporting the hypothesis that  $C_{60}$  does indeed have a closed-cage structure [3, 4]. Many reviews of endohedral fullerenes have been published, including a general review [5] and reviews of metallofullerenes [6, 7, 8], aspects related to interstellar endohedral fullerenes [9] and the effects of polarisability [10].

Endohedral fullerenes containing rare gas atoms (He, Ne, Ar) or some alkali metals can be formed in small quantities by bombarding empty fullerenes with ions having energies from  $\approx 6$  eV to  $\approx 50$  eV [11, 12] or treating fullerene powder under forced conditions [13]. Other endohedral fullerenes containing one or two atoms of rare gas, transition metal or alkali metal atoms can be formed using standard processes for the formation of fullerenes, such as laser graphite ablation or arc discharge [14, 6, 7, 15, 16]. Lists of the earliest-known endohedral fullerenes containing one or two encapsulated atoms, along with their methods of preparation, can be found in Ref. [17]. Fullerenes can also encapsulate larger clusters. For example, encapsulation of metallic clusters can stabilise giant fullerenes ( $C_{90}$  to  $C_{104}$ ) [18], and a novel planar quinary cluster can



be encapsulated inside  $C_{80}$  [19]. Very recently, a diuranium carbide cluster has been stabilised inside  $C_{80}$  [20].

A step-advance in endohedral fullerene science was made with the advent of a process known as molecular surgery [21, 22, 23, 24]. A chemical reaction is used to open a gap in a fullerene cage through which molecules can be inserted, after which a ‘reverse’ chemical reaction is used to close the gap. This allows larger molecules to be inserted than with the other methods, and at significantly higher yields. Molecules inserted into  $C_{60}$  this manner to date are  $H_2$  [24, 25, 26, 27], HD [27], HF [28] and  $H_2O$  [29, 30, 31]. Also, one and two molecules of  $H_2$  and  $H_2O$  have been inserted into  $C_{70}$  [32, 33]. Other works report situations in which a fullerene cage which is left open can incorporate He [34] or  $H_2$  [35], for example.

Encapsulation of other molecules has been considered *in silico* [36]. This includes the calculation of interaction energies, equilibrium geometries, dipole moments and harmonic vibrational frequencies [36], and determination of the effect on NMR parameters of encapsulating  $H_2$  and HD molecules [37].

Encapsulated molecules do not react chemically with fullerene cages (although simulations indicate that reactions may be possible under compression of  $H_2O@C_{60}$  in the direction of two opposing pentagons [38]). However, encapsulation of a metal atom inside a  $C_{60}$  molecule results in charge transfer from the metal atom to the  $C_{60}$  cage [16, 9, 5, 39, 40]. The charge transfer could be as much as 3 electrons in  $La@C_{60}$  [41]. Charge is also transferred to  $C_{82}$  in  $La@C_{82}$  and  $Y@C_{82}$  [14]. Calculations indicate that the charge transferred to a  $C_{60}$  cage upon encapsulation of light molecules is likely to be rather less, with the values reported being  $0.12e$  for CO,  $0.01e$  for  $CH_4$  and  $0.33e$  for  $CF_4$  [42]. For an isolated  $H_2O@C_{60}$  molecule, the extent of the charge transfer depends strongly on the method of calculation used, either ranging between  $0.01e$  and  $0.611e$  [43] or being around  $0.19e$  [44].

The issue of charge transfer is important when considering the possible presence of Jahn-Teller (JT) distortions. Neutral  $C_{60}$  contains a completely filled highest occupied molecular orbital (HOMO), so isolated  $C_{60}$  molecules are not subject to any JT effects. The  $C_{60}$  cage must be charged for a JT effect to operate. If sufficient charge is transferred, interactions between  $C_{60}$  molecules in solid samples containing endohedral fullerenes could stabilise a distortion due to cooperative JT effects [45, 46, 47]. It should be noted that the values for the charge transfer stated above are for isolated endohedral fullerene molecules. The charge transfer in clusters of molecules is unknown.

The question that arises is how any JT effect could be observed experimentally. It should be possible to observe signatures of any distortion of an endohedral fullerene cage using scanning tunnelling microscopy (STM), as for empty  $C_{60}$  molecules [48, 49, 50]. Although the displacements of the carbon atoms are too small to be detected directly, any reduction in symmetry due to the JT effect would split the molecular orbitals, resulting in a reduced set of states being imaged at a given energy. However, the endohedral fullerenes would need to be placed on a surface substrate in order to be imaged. Interactions with the surface substrate and alterations to the amount of charge transferred due to adsorption on a surface would complicate the interpretation of the results. STM imaging of  $H_2O@C_{60}$  on a NaCl substrate, either as single molecules or monolayers, has been carried out in an attempt to increase the charge transferred to the  $C_{60}$  cage. However, the results produced were identical to those of empty  $C_{60}$  molecules, with no evidence for any JT distortion [51]. No other relevant STM experiments appear to have been carried out to date. However, this doesn’t rule out the presence of JT distortions that are too small to detect in the STM experiments, or the presence of distortions in solid (powdered or polycrystalline) samples such as those used in INS. Hence other means of detecting the presence of any JT effect must be sought, such as through theoretical modelling or analysis of spectroscopic results.

## 2. Endohedral fullerenes potentially exhibiting JT effects

### 2.1. Endohedral fullerenes containing rare gas or metal atoms

Some quantum chemical computations indicate that there is a JT distortion in La@C<sub>60</sub> [41, 52]. Also, it has been proposed that for endohedral fullerenes doped with a rare gas or metal atom, a pseudo JT (PJT) coupling [53] can exist between  $T_{1u}$  electronic states of the C<sub>60</sub> molecule and  $H_u$  states of a rare gas or  $T_{1g}$  states of a metallic dopant, mediated by  $T_{1u}$  vibrations. This can lead to movement of the encapsulated atom away from the cage centre, and can also involve a distortion of the fullerene cage itself [54]. JT distortion of the fullerene cage to  $D_{5d}$  symmetry is necessary to be consistent with findings that the molecular symmetry of Ca@C<sub>60</sub> is  $C_{5v}$  [55].

### 2.2. Endohedral boron fullerenes

It has been predicted that encapsulation of various group V ligands into the hypothetical B<sub>80</sub> molecule can form donor-acceptor bonds with boron caps [56, 57]. There is a suggestion that JT effects may operate when a cluster of eight P atoms is encapsulated. The large size of this system tends to move eight boron caps outwards, whereas the PJT effect wants them to move inwards [56]. However, as B<sub>80</sub> has never been synthesised, there is no experimental evidence to confirm this observation.

It should be noted that when a methyne group is incorporated into the cage of a (hypothetical) B<sub>80</sub> molecule, DFT calculations support the idea that there is a PJT symmetry-breaking mechanism [56], in what has been called the substitutional JT effect. However, the methyne group in this case is part of the boron cage so this is not an endohedral fullerene.

### 2.3. Endohedral fullerenes containing light molecules

When light molecules such as H<sub>2</sub>, H<sub>2</sub>O, HD and HF are encapsulated inside a C<sub>60</sub> cage, there is substantial evidence that the environment seen by the encapsulated molecule in (poly)crystalline or powdered samples has a lower symmetry than the icosahedral symmetry of an undistorted C<sub>60</sub> molecule. In solid H<sub>2</sub>@C<sub>60</sub>, an observed specific heat anomaly [58] and analysis of the low-temperature dependence of INS spectra [59] both lead to the conclusion that the  $J = 1$  triplet state of *ortho*-H<sub>2</sub> is split by about 0.14 meV into a lower singlet and upper doublet. This is confirmed by IR absorption spectra of powder samples of H<sub>2</sub>@C<sub>60</sub> [60, 61], which indicate a splitting of about 0.12 meV [62]. In HF@C<sub>60</sub>, a splitting of around 0.48 meV is seen in the far- and mid-IR spectra of polycrystalline samples [28]. In highly pure samples of solid H<sub>2</sub>O@C<sub>60</sub>, INS revealed a splitting of the lowest *ortho*- $J = 1$  state of 0.48 meV into a lower singlet and upper doublet [31] (although the order of the splitting was incorrectly reported as having a doublet lowest [63]). Earlier INS and NMR studies had revealed a splitting of around 0.6 meV [29].

It has been suggested by several authors that the reduction in symmetry of the environment seen by an encapsulated molecule is due to a distortion of the cage of the encapsulating C<sub>60</sub> molecule [28, 29, 31, 59], possibly due to JT [28], JT-like [31] or analogous rotational effects [29]. Where the encapsulated molecule has a permanent electric dipole, it has been proposed that the symmetry reduction is due to interactions between dipoles in neighbouring cages [29, 31].

At temperatures below 90 K, solid C<sub>60</sub> has a simple cubic (space group  $Pa\bar{3}$ ) symmetry in which the C<sub>60</sub> molecules are locked into one of two orientations [64, 65], in a ratio of 5:1. In the dominant orientation, known as the P orientation, the double bond between two hexagons on one C<sub>60</sub> molecule face the centre of a pentagon on a neighbouring cage, such that each C<sub>60</sub> molecule has six double bonds and six pentagons facing its nearest neighbours. In the less-common ‘defect structure’ [17], known as the H orientation, the pentagonal faces are replaced by hexagonal faces. Very recently, the splittings in H<sub>2</sub>@C<sub>60</sub>, HF@C<sub>60</sub> and H<sub>2</sub>O@C<sub>60</sub> have all been explained using a model in which one filled C<sub>60</sub> molecule is surrounded by 12 empty C<sub>60</sub> molecules in either the P or H orientation, in order to mimic the structure of the complete solid [62, 66]. The cluster

has a point-group symmetry  $S_6$  [58]. As this symmetry only supports doublets and singlets (see e.g. Ref. [67]), it will necessarily cause splittings of degeneracies higher than two, such as the splittings of triplets into doublets and singlets. The mechanism determining the orderings and magnitudes of the splittings in the model of these authors involves electrostatic quadrupole interactions between the charge densities on the empty  $C_{60}$  molecules and the encapsulated molecule inside the central  $C_{60}$  molecule, with all of the  $C_{60}$  cages retaining their icosahedral symmetry.

It is possible that electric dipole-dipole interactions between water molecules in neighbouring  $C_{60}$  molecules could be partially responsible for the observed splitting of the  $J = 1$  level in  $H_2O@C_{60}$  even if the  $C_{60}$  cages retain their undistorted icosahedral geometries [68]. However, this interpretation requires the magnitude of the water dipole to be close to that for free water, rather than taking the expected screened value [68]. Therefore, it appears unlikely that this mechanism on its own can explain the observed splittings.

While the splittings in the  $J = 1$  state in light-molecule endohedral fullerenes can clearly be explained by a model involving electrostatic interactions between fullerenes in which the fullerene cages are undistorted, there are discrepancies between some of the predicted higher-energy states and those observed experimentally. The possibility that JT distortions of the fullerene cages are also taking place can certainly not be ruled out. JT distortions could operate alongside the proposed quadrupole interactions [62, 66], or even potentially instead of them.

From a symmetry point of view, theoretical calculations indicate that dynamic JT distortions of isolated  $C_{60}$  ions are expected to result in a distortion of the  $C_{60}$  cage to one of the subgroups  $\Gamma = D_{5d}, D_{3d}, D_{2h}$  or  $C_{2h}$  of  $I_h$  [69, 70, 71, 72, 73, 74, 75], with the results depending on both the charge state of the fullerene ion and the method of calculation used. Experimentally, analysis of the near and far infrared spectra of  $C_{60}^-$  anions indicates that the distortion is of  $D_{3d}$  symmetry [76]. Observation of the ultrafast decay rates of fullerene anions is also consistent with  $D_{3d}$  symmetry [77]. Of the four possible symmetries,  $D_{5d}$  and  $D_{3d}$  support doublet representations, so, in principle at least, a model involving distortions of the  $C_{60}$  cage to one of these two symmetries could provide the basis for an alternative model. Of course, JT distortions of isolated molecules are expected to be dynamic, with interconversion between equivalent lower-symmetry configurations taking place on a timescale of the order of pico or femto seconds [78]. However, it is possible that a distortion could be stabilised by the presence of the encapsulated water molecule or by cooperative JT effects between molecules.

As light-molecule endohedral fullerenes appear to be the most likely candidate for exhibiting JT effects, in the next section we will present results of a model involving distortions of the  $C_{60}$  cage in  $H_2O@C_{60}$  that explains the observed experimental results as least as well as the alternative model involving electrostatic interactions between (undistorted)  $C_{60}$  molecules [62, 66].

### 3. Model involving distortions of $C_{60}$ cages in $H_2O@C_{60}$

A free water molecule is a textbook example of an asymmetric top rotor, having different moments of inertia about its three principal axes. According to convention [79], the principal axes are labelled  $a$ ,  $b$  and  $c$ . The Hamiltonian of the asymmetric top rotor is written correspondingly in terms of rotational constants  $A_e$ ,  $B_e$  and  $C_e$  that are proportional to the inverse of the moment of inertia about the three principal axes, ordered such that  $A_e$  corresponds to rotation about the principal axis with the smallest moment of inertia and  $C_e$  to rotation about the axis with the largest moment of inertia. Figure 1 indicates the rotational axes of a water molecule associated with  $A_e$  and  $B_e$ .  $C_e$  corresponds to motion about an axis perpendicular to the plane of the water molecule.

The Hamiltonian for an asymmetric top rotor can be written in terms of any set of three angular momentum operators. There are  $3!$  ( $= 6$ ) ways of associating molecule-fixed axes

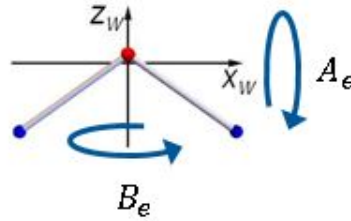


**Figure 1.** Principal axes of a free water molecule.

$\{x_w, y_w, z_w\}$  (through the centre of mass of the water molecule) with axes  $\{a, b, c\}$ . Depending on whether  $z_w$  is identified with  $a, b$  or  $c$ , the convention is known as type I, II or III. In addition, a superscript  $r$  or  $l$  is added depending on whether  $\{x_w, y_w, z_w\}$  is associated with a right or left-handed set of axes  $\{a, b, c\}$  (which is equivalent to associating  $\{x_w, y_w, z_w\}$  with a cyclic or anti-cyclic permutation of  $\{a, b, c\}$  respectively) [80]. Therefore, axes defined as in Figure 1 correspond to a  $\text{II}^l$  convention. In this convention, the rotational Hamiltonian is

$$\mathcal{H}_{\text{rot}} = \hbar^{-2} \left( A_e \hat{J}_x^2 + C_e \hat{J}_y^2 + B_e \hat{J}_z^2 \right) \quad (1)$$

where  $\{\hat{J}_x, \hat{J}_y, \hat{J}_z\}$  are components of the rotational angular momentum about the  $\{x_w, y_w, z_w\}$  axes. These can be written explicitly in terms of derivatives of Euler angles  $\{\phi, \theta, \chi\}$  [79].

The rotational levels that are eigenstates of Equation (1) are combinations of the eigenstates of the prolate ( $B_e = C_e$ ) and oblate ( $B_e = A_e$ ) symmetric tops [79]. The eigenstates are labelled  $J_{K_a, K_c}$  according to quantum numbers  $J, K_a$  and  $J, K_c$  of a prolate and oblate top respectively, as shown on the left and right-hand edges of Figure 2. The eigenstates in the two limits involve Wigner matrices  $D_{m, k_a}^{(J)}(\phi, \theta, \chi)$  and  $D_{m, k_c}^{(J)}(\phi, \theta, \chi)$  respectively, where  $K_a = |k_a|$  and  $K_c = |k_c|$ . The eigenvalues of the asymmetric top are shown in the figure as a function of  $\kappa = (2B_e - A_e - C_e)/(A_e - C_e)$ .

The rotational constants for a free water molecule are often taken to be those defined by Herzberg [81], namely  $A_e = 27.877 \text{ cm}^{-1}$ ,  $B_e = 14.512 \text{ cm}^{-1}$  and  $C_e = 9.285 \text{ cm}^{-1}$ . More recent *ab initio* calculations report very similar values, namely  $A_e = 27.8806 \text{ cm}^{-1}$ ,  $B_e = 14.5219 \text{ cm}^{-1}$  and  $C_e = 9.27753 \text{ cm}^{-1}$  or, when centrifugal distortion is taken into account,  $A_e = 27.8787 \text{ cm}^{-1}$ ,  $B_e = 14.5115 \text{ cm}^{-1}$  and  $C_e = 9.28799 \text{ cm}^{-1}$  [82]. Bunker and Jensen report rather different values of  $A_e = 27.2 \text{ cm}^{-1}$ ,  $B_e = 14.6 \text{ cm}^{-1}$  and  $C_e = 9.5 \text{ cm}^{-1}$  [79], although the source of these values is not stated. The rotational constants of Herzberg [81] and the centrifugally-corrected values of Császár *et al* [82] result in a value for  $\kappa$  of  $-0.438$ . This is shown as a vertical dashed line in Figure 2.

The rotational constants may change upon encapsulation. Indeed, the effective rotational constants for  $\text{CO}@C_{60}$  have been predicted to differ substantially from those of a free CO molecule [83]. Theoretical calculations report a slight elongation of the H-O bond length and slight reduction in bond angle upon encapsulation of a water molecule [22, 43, 84]. These geometrical changes suggest that the effective rotational constants may be slightly reduced upon encapsulation, although it is difficult to determine precise values for the effective constants of an encapsulated water molecule due to effects such as non-rigidity of the water molecule and anharmonicity in its vibrational motion. As the values aren't known, we will use the values of Herzberg [81] in the remainder of this paper.

There are several differences between the ideal and experimental INS spectra [31]. In particular, there are some small shifts in the positions of the energy levels, there are some additional excited states that can't be associated with those of a free water molecule and there

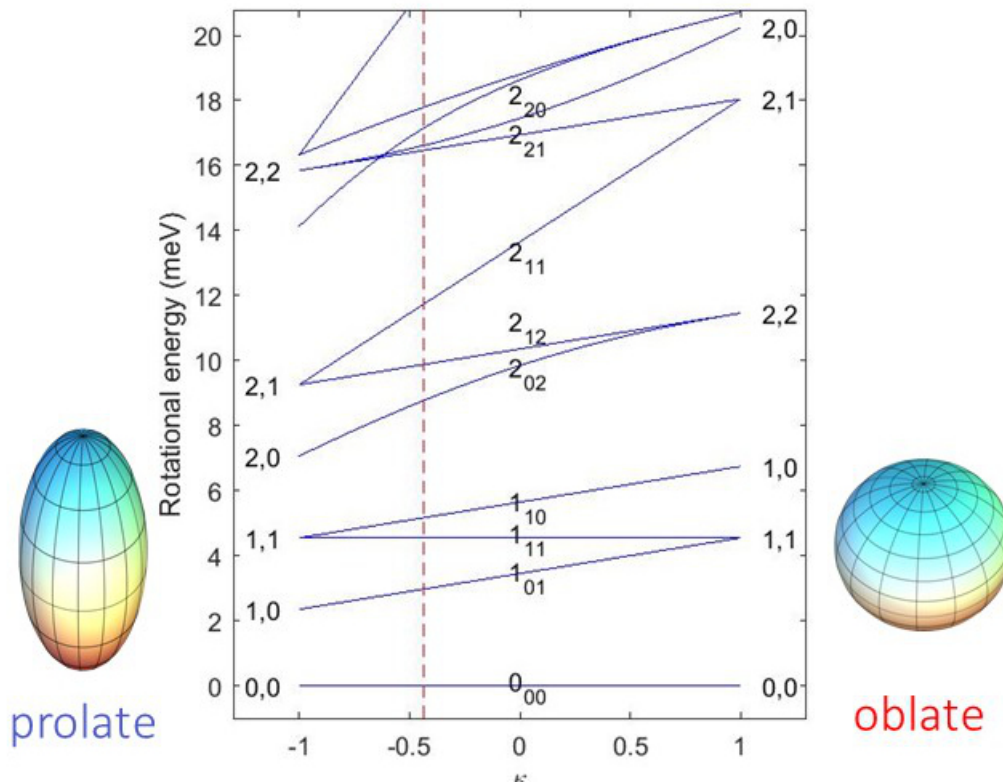


**Figure 2.** Rotational levels  $J_{K_a, K_c}$  of an asymmetric top molecule, in terms of quantum numbers  $J, K_a$  and  $J, K_c$  of prolate and oblate symmetric tops respectively. The dashed vertical line indicates the energy levels of a free water molecule.

is an obvious splitting in the  $1_{01}$  rotational level. There are probably also splittings in higher excited levels that can't be distinguished experimentally due to limitations in the resolution of the spectra. The small shifts in the energy levels could potentially arise due to changes in the rotational constants upon encapsulation. However, this would not introduce any splittings or result in any additional excited states.

The appearance of extra excited states can be attributed to quantisation of the rotational motion upon confinement. As the carbon atoms in an undistorted  $C_{60}$  molecule lie on the surface of a sphere, it is reasonable to assume that the potential that defines the translational motion of the centre of mass of the water molecule depends only on the distance,  $R_{cm}$ , of the centre of mass of the water molecule from the centre of the  $C_{60}$  molecule. Furthermore, it can be assumed that this potential is parabolic in  $R_{cm}$ . The translational Hamiltonian is then [85]

$$\mathcal{H}_{trans} = -\frac{\hbar^2}{2m}\nabla^2 + \frac{1}{2}m\omega^2 R_{cm}^2 \quad (2)$$

where  $m$  is the mass of the water molecule and  $\hbar\omega$  is the translational quantum. Comparison with the results of Density Functional Theory (DFT) calculations (see later) suggests that this is  $(18.1 \pm 0.1)$  meV. This is slightly smaller than the value of around 20.1 meV used in the series of papers by Felker and Bačić [86, 68, 62, 66], but larger than the value of around 15 meV expected for results involving  $D_2O$  [63]. The rotational levels are at energies  $(N + \frac{3}{2})\hbar\omega$ , where  $N$  is an integer.

Because the translational and rotational motions in Equations (1) and (2) are not coupled, the energy levels including

$$\mathcal{H}_{T+R} = \mathcal{H}_{\text{rot}} + \mathcal{H}_{\text{trans}} \quad (3)$$

are simply the pattern of rotational levels replicated for each translational level.

It is a little difficult to construct an energy level diagram from the INS data because the INS experiments report transitions between different energy levels, rather than simply energies relative to the ground state. They also include results from three different spectrometers that all have different resolutions. Slightly different energies are reported for the same transitions as measured with the different spectrometers. Table 8.1.6 of Ref. [87] gives energies and their associated errors as deduced from the data taking all information into account. These are the values that were plotted in Fig. 1 of Ref. [31]. The right-hand panel in Figure 3 reproduces these energy levels. The splitting in the triplet  $1_{01}$  level of 0.48 meV can be clearly seen. The experiments indicate that the upper component is a doublet and lower component is a singlet [63]. The left-hand panel shows the 12 lowest rotational levels associated with the ground state as solid blue lines. Confinement of the translational motion is seen via the dashed red lines, which show the lowest four rotational levels replicated for the first translation, taking the rotational quantum to be  $\hbar\omega = 18.1$  meV.

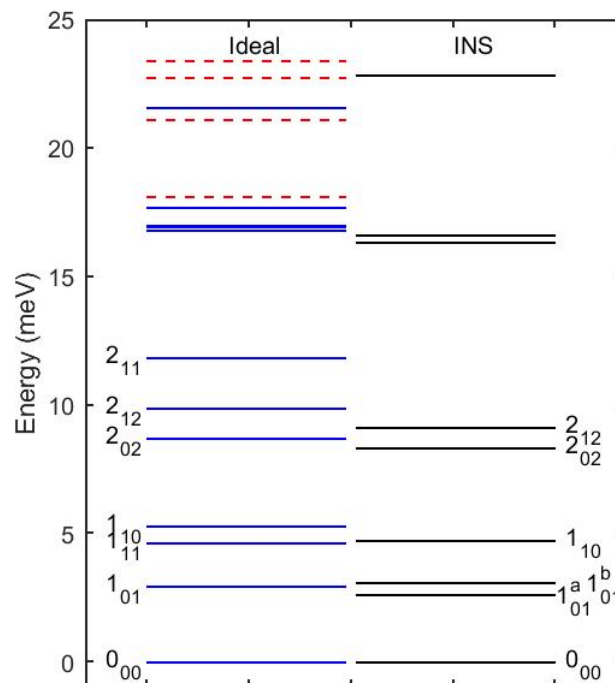


**Figure 3.** The panel on the left shows the energy levels of a confined water molecule taking into account translational and rotational motion only; the solid blue lines are the lowest 12 rotational levels associated with the lowest translational state, and the red dashed lines are rotational levels associated with the first excited translational state when the translational quantum  $\hbar\omega = 18.1$  meV. The rotational constants have been taken to be those of Herzberg [81]. Labels  $J_{K_a, K_c}$  are given for the low-lying levels. The panel on the right shows energy levels deduced from INS [31], along with the  $J_{K_a, K_c}$  assignments given in Ref. [31].

While there is clearly some correlation between the INS and calculated results, there are also some notable discrepancies. In particular, the splitting of the  $1_{01}$  level is not reproduced. This is to be expected, because  $\mathcal{H}_{T+R}$  does not contain any contributions that would lower the symmetry in order to cause a splitting. In addition, some of the calculated levels don't have experimental counterparts. The traditional view of inelastic neutron scattering is that all levels can be observed, with there being no selection rules governing allowed transitions. However, it has recently been shown that in spherical symmetry, transitions for which the Kronecker product of the symmetries of the initial and final state doesn't contain  $S_g, P_u, D_g, F_u \dots$  are forbidden [88]. In icosahedral symmetry, the transitions that would be forbidden in spherical symmetry are too weak to be observable experimentally. It is unclear how strong the transitions will be when there is a small distortion that lowers the symmetry below  $I_h$ . In addition, Goh *et al* report that *para*  $\leftrightarrow$  *para* transitions have negligible intensity at the level of sensitivity attained in the INS experiments [31]. Their Table 1 assign transitions from the *para* ground state  $0_{00}$  and the *ortho* ground state  $1_{01}$  to various excited states. These involve all of the  $J = 1$  and  $J = 2$  states except  $1_{10}$  and  $2_{11}$ .

The discrepancies in the INS spectra indicate that the water molecule is sensitive to the environment in which it is encapsulated. If the water molecule experiences an icosahedral ( $I_h$ ) environment (consistent with the symmetry of an undistorted  $C_{60}$  molecule), degeneracies higher than 5 are lifted but the  $1_{01}$  level will not split into a singlet and a doublet. This must be the case because doublet representations are not supported in  $I_h$  symmetry, and a symmetry analysis of the triplet  $1_{01}$  level shows that it can't be split into three singlets with an accidental degeneracy.

The fact that the  $1_{01}$  level remains unsplit in  $I_h$  symmetry was illustrated explicitly in calculations in which states were written using a total angular momentum for the translations and rotations, combined with a Lennard-Jones (L-J) 12-6 potential to model the interaction between a rigid water molecule and a rigid  $C_{60}$  cage [86]. The result can be seen as representing translation-rotation (TR) coupling because the Hamiltonian does not separate into translational and rotational parts. As would be expected from symmetry considerations, these calculations did not lift the degeneracy of any of the low-lying rotational states.

As stated above, the reduction in symmetry seen by the water molecule could be due to JT distortions which could potentially be of  $D_{5d}, D_{3d}, D_{2h}$  or  $C_{2h}$  symmetry.  $D_{2h}$  and  $C_{2h}$  symmetries only support singlets, whereas  $D_{5d}$  and  $D_{3d}$  symmetries support doublets. Hence  $D_{5d}$  and  $D_{3d}$  are the most likely candidates for explaining the observed splitting of the  $1_{01}$  level. Alternatively, the symmetry reduction could be to  $S_6$  symmetry due to interactions with neighbouring (icosahedral)  $C_{60}$  molecules [62, 66].

As the states of an encapsulated water molecule must also have a defined parity under exchange of the two H atoms, the symmetry groups under consideration should actually be the direct product of the point group concerned and the permutation group  $S_2$ . The product involving the icosahedral group, originally developed to describe the symmetry of the TR Hamiltonian in  $H_2@C_{60}$  [88] and then applied to  $H_2O@C_{60}$  [86], has been called  $I_h^{(12)}$ . Similar notation can therefore be used for the lower symmetry groups. The irreducible representations (irreps.) are labelled  $\Gamma^{(s)}$  if the states are invariant under exchange of the two H atoms, and  $\Gamma^{(a)}$  if they change sign.

Instead of incorporating TR coupling via a L-J potential, TR coupling can be incorporated in general terms from symmetry considerations alone. According to fundamental rules of quantum mechanics, the Hamiltonian describing a system must be invariant under all operations of the group to which the system belongs [89]. Therefore, it is possible to construct a Hamiltonian to reflect a reduction in symmetry of the  $C_{60}$  cage from  $I_h$  to one of its subgroups by taking linear combinations of products of translational and rotational basis states that transform according to the totally-symmetric representation  $\Gamma^{(s)}$  in the required subgroup symmetry ( $A_g^{(s)}$  in  $I_h^{(12)}$  and  $S_6^{(12)}$  symmetries, or  $A_{1g}^{(s)}$  in  $D_{5d}^{(12)}$  and  $D_{3d}^{(12)}$  symmetries for example).

In order to calculate the energies of TR-coupled states including the symmetry-lowering perturbation, it is useful to derive a basis of TR-coupled states that transform according to the required symmetry. Although not essential, calculating matrix elements of the total Hamiltonian  $\mathcal{H}_{\text{tot}}$  ( $= \mathcal{H}_{\text{T+R}}$  plus the symmetry-lowering perturbation) in the symmetry-adapted basis produces a block-diagonal matrix in which the resulting energy levels are automatically associated with the irrep. to which they belong, including being labelled as symmetric or antisymmetric under exchange of the H atoms. The totally-symmetric states that are required to form the symmetry-lowering perturbation are also generated as part of this process.

Symmetry-adapted states can be obtained using the method of projection operators [90]. This has previously been used to obtain vibronic states for  $T \otimes (e + t_2)$  and  $T \otimes h$  JT systems from products of electronic and vibrational states [91, 69] associated with geometrically-equivalent distorted configurations that have the same energy as each other. The procedure here is similar, except that the basis states contain products of translational and rotational states associated with geometrically-equivalent positions of the water molecule, rather than products of electronic and vibrational states. An example showing one possible set of geometrically-equivalent positions of the water molecule with respect to a truncated icosahedron is illustrated in Figure 4.

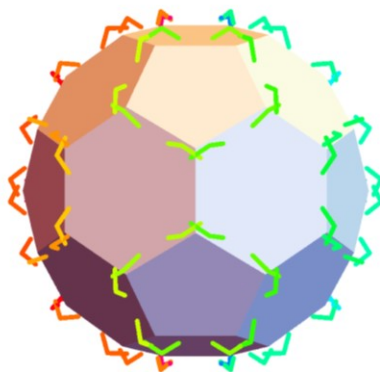


**Figure 4.** An example of geometrically-equivalent positions of a water molecule with respect to a truncated icosahedron.

The rotational parts of the basis states are written in terms of the Wigner matrices  $D_{m,k}^{(J)}(\phi, \theta, \chi)$ . The translational parts of the basis states are written in terms of spherical harmonics  $Y_{l,m}(\theta_{\text{cm}}, \phi_{\text{cm}})$  and radial functions  $\phi_{N_r,l}(R_{\text{cm}})$  involving the spherical polar coordinates  $\{R_{\text{cm}}, \theta_{\text{cm}}, \phi_{\text{cm}}\}$  of the centre of mass of the water molecule relative to the centre of the (undistorted)  $\text{C}_{60}$  molecule.  $N_r$  is an integer ( $\geq 0$ ) defined such that the translational energy levels are  $(N + \frac{3}{2})\hbar\omega$ , where  $N = 2N_r + l$  [85].

As the totally symmetric symmetry adapted states  $\Gamma^{(s)}$  ( $\Gamma = A_g$  or  $A_{1g}$ ) will be used to form a perturbation, it is useful to analyse them in more detail. It is found that in  $D_{5d}^{(12)}$  symmetry, the results consist of four contributions that actually have spherical symmetry and nine contributions that have spheroidal ( $D_{\infty h}^{(12)}$ ) symmetry. The spherical contributions also occur in  $I_h^{(12)}$  symmetry. The fact that the states have an accidentally higher symmetry than that of the group used to derive them reflects the fact that the carbon atoms lie on the surface of a sphere when the cage is undistorted, or on the surface of a spheroid when it is distorted, with the results in both cases being insensitive to the positions of the carbon atoms. The results

for  $D_{3d}^{(12)}$  symmetry are the same as those for  $D_{5d}^{(12)}$  but with some additional contributions that do not occur in  $D_{5d}^{(12)}$  symmetry. Likewise, the results for  $S_6^{(12)}$  symmetry are the same but with even more additional contributions.

By careful manipulation using relations between products of Wigner matrices and orthogonality relations between both Wigner matrices and spherical harmonics, it is possible to determine analytical expressions for all of the matrix elements of  $\mathcal{H}_{\text{tot}}$ , up to chosen maximum values for  $J$  and  $l$ , in terms of constants  $k_{i,N_r}$  multiplying the  $i$  different contributions to the potential for each value of  $N_r$ . For any given values of the  $k_{i,N_r}$ , it is a simple matter to diagonalise the resulting block-diagonal matrices to find the energies of the states including the effect of the symmetry-lowering perturbation, and to label the results according to the relevant irreps.

While a symmetry analysis can be used to determine the *form* of the symmetry-lowering potential, it can't be used to obtain values for the coefficients. Therefore, values for the  $k_{i,N_r}$  must be determined by other means. Values for the coefficients of the spherical terms can be obtained by equating the variation in energy as the water molecule moves along various radial directions through the centre of an undistorted  $C_{60}$  molecule with the energy obtained from DFT calculations involving a rigid water molecule moving inside a rigid  $C_{60}$  cage. Calculations using the hybrid Gaussian plane waves method (GPW) that account for non-covalent interactions and long-range correlation corrections, as implemented in CP2K [92], show that the variation in energy when the water molecule has its dipole axis  $z_{\text{cm}}$  aligned along a  $C_2$  axis and its centre of mass moves along an  $x_{\text{cm}}$  axis is approximately symmetric about the centre of the  $C_{60}$  molecule, but is flatter nearer the centre than would be obtained for a parabolic potential alone. This confirms that it is necessary to include TR-coupling contributions even if the  $C_{60}$  molecule doesn't distort from icosahedral. When the centre of mass moves along the  $z_{\text{cm}}$  direction, the potential is clearly asymmetric about the origin, due to differences in the placement of the carbon atoms relative to the water molecule at positive and negative values of  $z_{\text{cm}}$  in this geometry. Results for both geometries are shown in Figure 5.

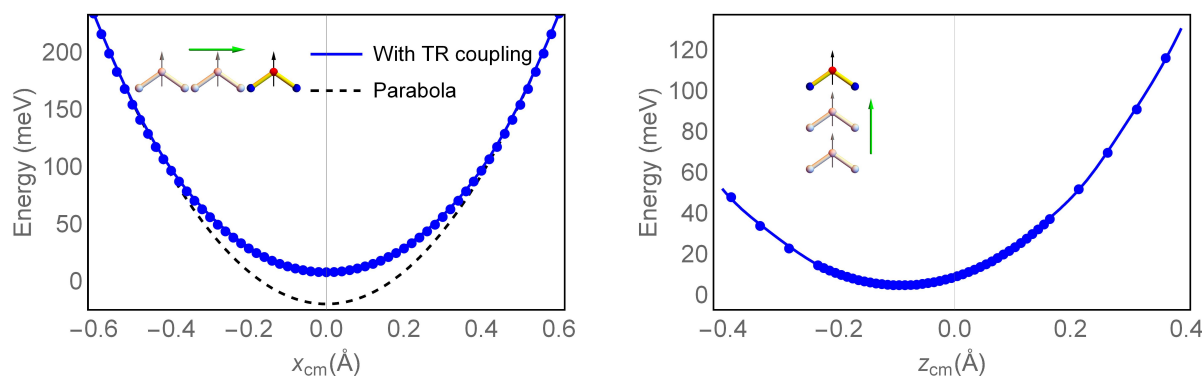


**Figure 5.** Variation in energy as determined by DFT (solid blue circles) as a water molecule moves along axes  $x_{\text{cm}}$  (left) and  $z_{\text{cm}}$  (right). The black dashed line indicates the potential that would be obtained from the parabolic potential in the translational Hamiltonian alone, assuming that the translational quantum is  $\hbar\omega = 18.1$  meV. The solid blue lines are fits of the energy to the parabolic potential and the TR-coupling perturbation.

Although the potential that lowers the symmetry to  $D_{\infty h}^{(12)}$  contains 13 terms, only two of these terms contribute when the problem is restricted to consideration of the lowest translational state

only. The other terms contribute via mixing between the lowest translational state and higher translational states, and/or within the higher translational states. As the translational quantum is  $\approx 18.1$  meV, it can be expected that the effect of this mixing on the  $J = 1$  states and the  $2_{02}$  and  $2_{12}$  states, which are all less than 10 meV above the ground state, will be very small. This has been confirmed by explicit calculations, that show that the effect of higher-order terms on these states is negligible for values of the coefficients that are of the order of magnitude required to match the INS data. Hence an attempt can be made to match the low-lying energy levels observed in INS by considering the lowest translation and varying two parameters only.

By varying the two parameters in the potential that includes contributions of spherical and  $D_{\infty h}^{(12)}$  symmetries, it is possible to get an identical match to the  $J = 1$  energies as reported in Ref. [66] where the symmetry-lowering was taken to be due to electrostatic interactions between the electron density of the water molecule and that of neighbouring (icosahedral)  $C_{60}$  molecules. This is somewhat surprising, as the model used in Ref. [66] assumed that the effective symmetry seen by the water molecule is  $S_6$ . This shows that it is spheroidal contributions to the overall reduction in symmetry that are responsible for producing the energies of the  $J = 1$  levels at least.

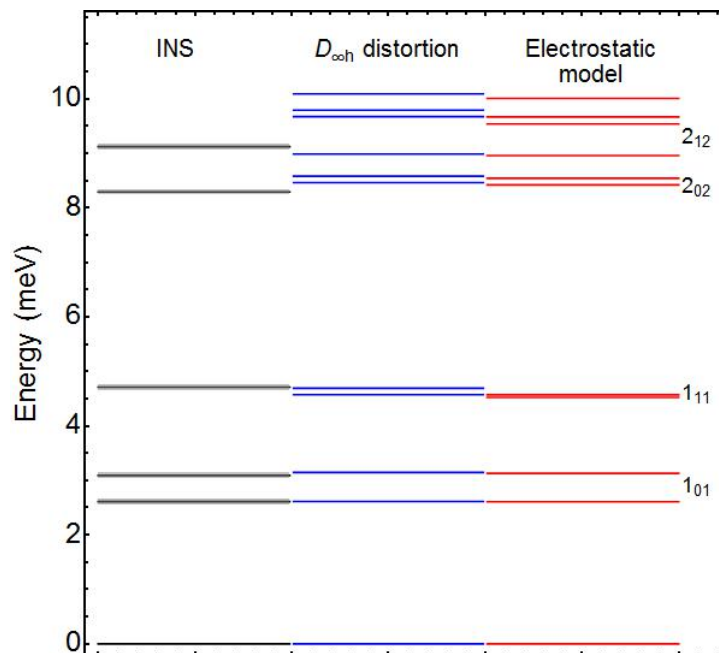


**Figure 6.** The energy levels on the left are all those below 10 meV as deduced from INS [31, 87], with grey boxes indicating the stated experimental uncertainties. The middle column shows one possible set of the calculated energy levels of a confined water molecule including TR coupling with spheroidal distortions to the  $C_{60}$  cage, excluding the (split)  $1_{10}$  level (which is not seen in INS) and with rotational constants as in Figure 3. The column on the right shows result taken from Ref. [66].

The left-hand column in Figure 6 shows the low-lying energy levels (below 10 meV) as deduced from the INS transitions [31, 87], with grey boxes indicating the experimental uncertainties, and the right-hand column shows the relevant energy levels from the electrostatic model [66]. It can be seen that the  $1_{01}$  levels are matched almost exactly, with a slight overestimation of

the splitting. However, there are some discrepancies in the higher levels. As stated above, the spheroidal-distortion model can give the same results as those on the right. However, by choosing different values for the two free parameters, it is possible to still get the same matches to the  $1_{01}$  levels as with the electrostatic model but to give slightly different results for the other levels. One such possibility that gives marginally better results for the  $1_{11}$  levels is shown in the middle column of the figure. However, the agreement with the  $2_{02}$  and  $2_{12}$  levels is not exact in either model. Note that the  $1_{10}$  levels have been omitted from both the middle and right-hand columns as these levels are not observed in INS. Note also that an exact match to both of the  $1_{01}$  levels can be obtained by reducing the value of the rotational constant  $C_e$  by a very small amount.

#### 4. Conclusions

We have examined the evidence for whether observable JT effects might be present in various endohedral fullerenes. This shows that the most likely candidates are  $C_{60}$  fullerenes encapsulating a light molecule such as  $H_2$  or  $H_2O$ , where experimental measurements show splittings in one of the low-lying energy levels. This indicates that the encapsulated molecules are subject to an environment with a symmetry lower than the icosahedral symmetry of the  $C_{60}$  cage. However, this evidence on its own does not reveal the physical origin of the symmetry reduction.

Our calculations on  $H_2O@C_{60}$  have shown that the low-lying INS results can be explained using a model in which the encapsulated water molecule experiences an environment of spheroidal ( $D_{\infty h}$ ) symmetry. The origin of the distortion could be the JT effect. In this case, the distortions would probably be of  $D_{5d}$  or  $D_{3d}$  symmetry, with the distortion axis coinciding with a 5 or 3-fold axis of the  $C_{60}$  molecule respectively. This would manifest itself as the higher  $D_{\infty h}$  symmetry. However, it is not expected that the water molecule would be able to follow rapid distortions of the  $C_{60}$  cage as required by a dynamic JT effect. There would need to be a mechanism to stabilise a distortion of the  $C_{60}$  cage, such as through cooperative interactions between  $C_{60}$  molecules in an intermolecular JT effect. Also, it would be necessary for sufficient charge to be transferred to the  $C_{60}$  cage such that a JT effect could occur. Alternatively, it could be that the origin of the distortion is due to electrostatic interactions between an encapsulated water molecule and neighbouring (icosahedral)  $C_{60}$  cages [62, 66]. In this case, the effective symmetry is  $S_6$  but again the evidence is that it would manifest itself as  $D_{\infty h}$ . Of course, it could be that both JT effects and electrostatic interactions play a role in determining the observed energy splittings, with both mechanisms contributing in such a way that the important distortional terms are of  $D_{\infty h}$  symmetry.

In order to determine the respective roles of JT effects and electrostatic interactions in light-molecule endohedral fullerenes, further calculations involving higher excited states will be required alongside further high-resolution experimental measurements.

#### Acknowledgments

ER is grateful for funding from Umm Al-Qura University. We also acknowledge the support of the University of Nottingham High Performance Computing Facility (in particular, Dr Colin Bannister).

#### References

- [1] Kroto H W, Heath J R, O'Brien S C, Curl R F and Smalley R E 1985 *Nature* **318** 162–3
- [2] Heath J R, O'Brien S C, Zhang Q, Liu Y, Curl R F, Kroto H W, Tittel F K and Smalley R E 1985 *J. Am. Chem. Soc.* **107** 7779–80
- [3] O'Brien S C, Heath J R, Curl R F and Smalley R E 1988 *J. Chem. Phys.* **88** 220–30
- [4] Weiss F D, Elkind J L, O'Brien S C, Curl R F and Smalley R E 1988 *J. Am. Chem. Soc.* **110** 4464–5

- [5] Delgado J L, Filippone S, Giacalone F, Herranz M A, Illescas B, Perez E M and Martin N 2014 *Buckyballs (Topics in Current Chemistry vol 350)* (Berlin: Springer-Verlag Berlin) pp 1–64
- [6] Lu X, Feng L, Akasaka T and Nagase S 2012 *Chem. Soc. Rev.* **41** 7723–60
- [7] Cong H L, Yu B, Akasaka T and Lu X 2013 *Coord. Chem. Rev.* **257** 2880–98
- [8] Lu X, Bao L P, Akasaka T and Nagase S 2014 *Chem. Commun.* **50** 14701–15
- [9] Omont A 2016 *Astron. Astrophys.* **590** A52
- [10] Sabirov D S 2014 *RSC Adv.* **4** 44996–5028
- [11] Campbell E E B, Ehlich R, Heusler G, Knospe O and Sprang H 1998 *Chem. Phys.* **239** 299–308
- [12] Deng R, Clegg A and Echt O 2003 *Int. J. Mass Spectrom.* **223** 695–701
- [13] Saunders M, Jimenezvazquez H A, Cross R J and Poreda R J 1993 *Science* **259** 1428–30
- [14] Shinohara H 2000 *Rep. Prog. Phys.* **63** 843–92
- [15] Dunk P W, Adjizian J J, Kaiser N K, Quinn J P, Blakney G T, Ewels C P, Marshall A G and Kroto H W 2013 *Proc. Natl. Acad. Sci.* **110** 18081–6
- [16] Dunk P W, Mulet-Gas M, Nakanishi Y, Kaiser N K, Rodríguez-Fortea A, Shinohara H, Poblet J M, Marshall A G and Kroto H W 2014 *Nat. Commun.* **5** 5844
- [17] Dresselhaus M S, Dresselhaus G and Eklund P C 1996 *Science of Fullerenes and Carbon Nanotubes* (San Diego: Academic Press)
- [18] Bao L P, Peng P and Lu X 2018 *Acc. Chem. Res.* **51** 810–15
- [19] Wang T S, Feng L, Wu J Y, Xu W, Xiang J F, Tan K, Ma Y H, Zheng J P, Jiang L, Lu X, Shu C Y and Wang C R 2010 *J. Am. Chem. Soc.* **132** 16362–4
- [20] Zhang X X *et al* 2018 *Nat. Commun.* **9** 8
- [21] Murata M, Murata Y and Komatsu K 2008 *Chem. Commun.* **46** 6083–94
- [22] Kurotobi K and Murata Y 2011 *Science* **333** 613–6
- [23] Hashikawa Y, Murata M, Wakamiya A and Murata Y 2016 *Organic Letters* **18** 6348–51
- [24] Komatsu K 2013 *Philos. Trans. Royal Soc. A* **371** 1–3
- [25] Komatsu K, Murata M and Murata Y 2005 *Science* **307** 238–40
- [26] Matsuo Y, Isobe H, Tanaka T, Murata Y, Murata M, Komatsu K and Nakamura E 2005 *JACS* **127** 17148–9
- [27] Horsewill A J *et al.* 2010 *Phys. Rev. B* **82** 081410
- [28] Krachmalnicoff A *et al.* 2016 *Nat. Chem.* **8** 953–7
- [29] Beduz C *et al.* 2012 *Proc. Natl. Acad. Sci.* **109** 12894–8
- [30] Mamone, S *et al* 2014 *J. Chem. Phys.* **140** 194306
- [31] Goh K S K *et al.* 2014 *Phys. Chem. Chem. Phys.* **16** 21330–9
- [32] Murata M, Maeda S, Morinaka Y, Murata Y and Komatsu K 2008 *J. Am. Chem. Soc.* **130** 15800–1
- [33] Zhang R, Murata M, Aharen T, Wakamiya A, Shimoaka T, Hasegawa T and Murata Y 2016 *Nat. Chem.* **8** 435–41
- [34] Stanisky C M, Cross J, Cross R J, Saunders M, Murata M, Murata Y and Komatsu K 2005 *JACS* **127** 299–302
- [35] Sawa H, Wakabayashi Y, Murata Y, Murata M and Komatsu K 2005 *Angewandte Chemie-International Edition* **44** 1981–3
- [36] Dolgonos G A and Peslherbe G H 2014 *Phys. Chem. Chem. Phys.* **16** 26294–305
- [37] Jankowska M, Kupka T and Stobinski L 2015 *J. Mol. Graph.* **62** 26–37
- [38] Sabirov D S 2013 *J. Phys. Chem. C* **117** 1178–82
- [39] Cioslowski J and Fleischmann E D 1991 *J. Chem. Phys.* **94** 3730–4
- [40] Kroto H W and Jura M 1992 *Astron. Astrophys.* **263** 275–80
- [41] Slanina Z, Lee S L, Adamowicz L, Uhlik F and Nagase S 2005 *Int. J. Quantum Chem.* **104** 272–7
- [42] Marenich A V, Cramer C J and Truhlar D G 2013 *Chem. Sci.* **4** 2349–56
- [43] Varadwaj A and Varadwaj P R 2012 *Chem. Eur. J.* **18** 15345–60
- [44] Oliveira O and Gonçalves A 2014 *Computational Chemistry* **2** 51–8
- [45] Sobolewski A L 1997 *Chem. Phys. Lett.* **267** 452–9
- [46] Dunn J L 2004 *Phys. Rev. B* **69** 064303
- [47] Moujaes E A and Dunn J L 2010 *J. Phys.: Condens. Matter* **22** 085007
- [48] Hands I D, Dunn J L and Bates C A 2010 *Phys. Rev. B* **82** 155425
- [49] Dunn J L, Lakin A J and Hands I D 2012 *New J. Phys.* **14** 083038
- [50] Dunn J L, Alqannas H S and Lakin A J 2015 *Chem. Phys.* **460** 14–25
- [51] Leaf J 2017 *A study of C<sub>60</sub> assemblies via Scanning Probe microscopy, Hückel and Monte Carlo methods* Ph.D. thesis University of Nottingham, UK
- [52] Slanina Z, Uhlik F, Lee S L and Adamowicz L 2003 *J. Low Temp. Phys.* **131** 1259–63
- [53] Bersuker I B 2016 *Spontaneous symmetry breaking in matter induced by degeneracies and pseudodegeneracies* vol 160 (John Wiley and Sons) pp 159–208

- [54] Clougherty D P and Anderson F G 1998 *Phys. Rev. Lett.* **80** 3735–8
- [55] Wang L S, Alford J M, Chai Y, Diener M, Zhang J, McClure S M, Guo T, Scuseria G E and Smalley R E 1993 *Chem. Phys. Lett.* **207** 354–9
- [56] Muya J T, Gopakumar G, Lijnen E, Nguyen M T and Ceulemans A 2012 Investigations of the boron buckyball  $b_{80}$ : Bonding analysis and chemical reactivity *Vibronic Interactions and the Jahn-Teller Effect: Theory and Applications (Progress in Theoretical Chemistry and Physics vol 23)* ed Atanasov M, Daul C and Tregenna Piggott P L W (Dordrecht: Springer) pp 265–78
- [57] Muya J T, Lijnen E, Minh T N and Ceulemans A 2011 *J. Phys. Chem. A* **115** 2268–80
- [58] Kohama, Y *et al* 2009 *Phys. Rev. Lett.* **103** 073001
- [59] Mamone S, Johnson M R, Ollivier J, Rols S, Levitt M H and Horsewill A J 2016 *Phys. Chem. Chem. Phys.* **18** 1998–2005
- [60] Mamone S *et al.* 2009 *J. Chem. Phys.* **130** 081103
- [61] Rõõm T *et al* 2013 *Philos. Trans. R. Soc. A-Math. Phys. Eng. Sci.* **371** 20110631
- [62] Felker P M, Vlček V, Hietanen I, FitzGerald S, Neuhauser D and Bačić Z 2017 *Phys. Chem. Chem. Phys.* **19** 31274–83
- [63] Horsewill A J 2017 Private communication
- [64] Copley J R D, Neumann D A, Cappelletti R L and Kamitakahara W A 1992 *J. Phys. Chem. Solids* **53** 1353–71
- [65] FitzGerald S A, Yildirim T, Santodonato L J, Neumann D A, Copley J R D, Rush J J and Trouw F 1999 *Phys. Rev. B* **60** 6439–51
- [66] Bačić Z, Vlček V, Neuhauser D and Felker P M 2018 *Faraday Discussions* In press
- [67] Jacobs P 2005 *Group theory with applications in chemical physics* (Cambridge: Cambridge University Press)
- [68] Felker P M and Bačić Z 2017 *J. Chem. Phys.* **146** 084303
- [69] Dunn J L and Bates C A 1995 *Phys. Rev. B* **52** 5996–6005
- [70] Ceulemans A and Fowler P W 1990 *J. Chem. Phys.* **93** 1221–34
- [71] O'Brien M C M 1996 *Phys. Rev. B* **53** 3775–89
- [72] Chancey C C and O'Brien M C M 1997 *The Jahn-Teller effect in  $C_{60}$  and other icosahedral complexes* (Princeton: Princeton University Press)
- [73] Ramanantoanina H, Gruden-Pavlović M, Zlatar M and Daul C 2012 *Int. J. Quantum Chem.* **113** 802–7
- [74] Ramanantoanina H, Zlatar M, García-Fernández P, Daul C and Gruden-Pavlović M 2013 *Phys. Chem. Chem. Phys.* **15** 1252–9
- [75] Alqannas H S, Lakin A J, Farrow J A and Dunn J L 2013 *Phys. Rev. B* **88** 165430
- [76] Hands I D, Dunn J L, Bates C A, Hope M J, Meech S R and Andrews D L 2008 *Phys. Rev. B* **77** 115445
- [77] Hope M J, Higglet M P, Andrews D L, Meech S R, Hands I D, Dunn J L and Bates C A 2009 *Chem. Phys. Lett.* **474** 112–4
- [78] Hands I D, Dunn J L and Bates C A 2006 *Phys. Rev. B* **73** 235425
- [79] Bunker P R and Jensen P 2005 *Fundamentals of Molecular Symmetry* (Bristol: IOP Publishing)
- [80] King G W, Hainer R M and Cross P C 1943 *J. Chem. Phys.* **11** 27–42
- [81] Herzberg G 1966 *Molecular Spectra & Molecular Structure III (Polyatomic Molecules)* (New Jersey: Van Nostrand)
- [82] Császár A G, Czako G, Furtenbacher T, Tennyson J, Szalay V, Shirin S V, Zobov N F and Polyansky O L 2005 *J. Chem. Phys.* **122** 214305
- [83] Olthof E H T, van der Avoird A and Wormer P E S 1996 *J. Chem. Phys.* **104** 832–47
- [84] Farimani A B, Wu Y and Aluru N R 2013 *Phys. Chem. Chem. Phys.* **15** 17993–18000
- [85] Flügge S 1974 *Practical Quantum Mechanics* (Berlin: Springer-Verlag)
- [86] Felker P M and Bačić Z 2016 *J. Chem. Phys.* **144** 201101
- [87] Goh K S K 2015 *Spectroscopic investigation of the quantum dynamics of small molecules encapsulated inside fullerene cages* Ph.D. thesis University of Nottingham, UK
- [88] Poirier B 2015 *J. Chem. Phys.* **143** 101104
- [89] Bransden B and Joachain C 1989 *Introduction to Quantum Mechanics* (Harlow, England: Longman Scientific and Technical)
- [90] Bradley C J and Cracknell A P 1972 *The Mathematical Theory of Symmetry in Solids* (New York: Oxford University Press Inc)
- [91] Hallam L D, Bates C A and Dunn J L 1992 *J. Phys.: Condens. Matter* **4** 6775–96
- [92] The CP2K Developers Group 2013 CP2K ver 2.4.0 <https://www.cp2k.org/>